URSI GASS 2021, Rome, Italy, 28 August - 4 September 2021

Teaching Directional Couplers and Directional Bridges

Carlo Carobbi
Department of Information Engineering, University of Florence, Firenze, ITALY

Abstract

Directional couplers and bridges are used as components of measurement chains to monitor forward and reflected power in conducted and radiated measurements or as building blocks of measuring instruments like scalar and vector network analyzers. In my experience as a master's degree and PhD student these devices were presented, at most, for the purpose of illustrating the principle of operation but without any mention of their metrological characteristics and limits of accuracy. The scope of this contribution is to discuss, after having introduced the principle of operation, the essential metrological characteristics of coaxial directional couplers and resistive directional bridges, namely coupling, isolation, directivity, insertion loss and mismatch and provide the basic equations useful to quantify errors in measurement of forward and reflected power.

1 Introduction

The problem of accurately measuring forward and reflected waves has great importance in modern radiofrequency applications. Efficient use of radiofrequency energy by portable (wearable) devices, integrity of signals over high-speed digital connections, testing immunity of large systems by generating strong electromagnetic fields are all applications that require impedance matching, over a large bandwidth and power range. Education in radiofrequency metrology cannot overlook this important topic, also because measuring instruments that permit to implement the reflectometric measurement techniques (spectrum analyzers and vector network analyzers) are nowadays much more affordable and widespread than in the past. The scope here is to illustrate how metrological concepts related to reflectometric measurement can be introduced to master's degree students in electronics and communications engineering. This contribution is in the vein of several recent papers of the same author devoted to the quality of testing and calibration in the specific sector of electromagnetic compatibility [1-21].

2 Directional Couplers

Directional couplers are realized by coupling two transmission lines (e.g. coaxial or stripline). To understand the principle of operation of directional couplers we consider the mutual coupling between lossless transmission lines in a homogenous dielectric medium, see Fig. 1. The speed of propagation of waves is v. The lines have length L. The per-unit-length parameters of the lines are self-inductances, l_G and l_R, mutual inductance, l_m, capacitances, c_G and c_R, and mutual capacitance, c_m.

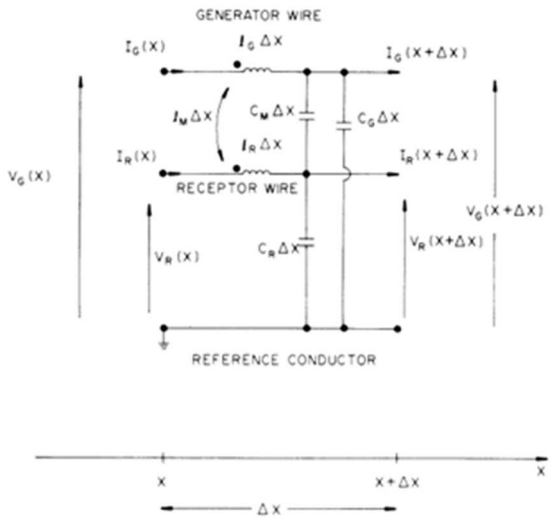

Figure 1. Lumped model of a short section of three-conductor transmission line (reproduced from [22], Fig. 3).

We have

$$\mathbf{L}=\begin{bmatrix} l_G & l_m \\ l_m & l_R \end{bmatrix}, \quad \mathbf{C}=\begin{bmatrix} c_G+c_m & -c_m \\ -c_m & c_R+c_m \end{bmatrix}. \tag{1}$$

Matrices $\mathbf{L}$ and $\mathbf{C}$ are related due to TEM propagation and we have

$$\mathbf{LC}=\begin{bmatrix} 1/v^2 & 0 \\ 0 & 1/v^2 \end{bmatrix}. \tag{2}$$

Note that if the speed of propagation v is known then the capacitance matrix $\mathbf{C}$ can be obtained from inductance matrix $\mathbf{L}$ and vice versa. Substituting (1) into (2) and assuming that the lines are identical ($l_R=l_G=l$ and $c_R=c_G=c$) we obtain

$$\begin{cases} l\left(c+c_m\right)-l_m c_m=\dfrac{1}{v^2} \\ -lc_m+l_m\left(c+c_m\right)=0 \end{cases}. \tag{3}$$

From (3) we obtain

$$\begin{cases} v=\dfrac{1}{\sqrt{1+k}}\dfrac{1}{\sqrt{lc}} \\ \dfrac{l_m}{l}=\dfrac{c_m}{c+c_m} \end{cases}. \tag{4}$$

Wavelength is $\lambda=v/f$, where f is frequency, and the wavenumber is $\beta=2\pi/\lambda$. We define the mutual coupling factor k as

$$k=\frac{l_m}{l}=\frac{c_m}{c+c_m}. \tag{5}$$

We assume that line G is fed by a voltage source at the left side and terminated by a load at the right side. The other line R is terminated by a load at both left and right sides. The internal resistance of the source and the loads are equal to Z_0, where

$$Z_0 = \sqrt{\frac{l}{c + c_m}} = vl\sqrt{1-k^2} \tag{6}$$

represents the characteristic impedance of each line when coupled to the other line. We obtain the following equations for coupled lines

$$\begin{aligned} \frac{d}{dx}\mathbf{V}(x) &= -\mathbf{Z}\mathbf{I}(x) \\ \frac{d}{dx}\mathbf{I}(x) &= -\mathbf{Y}\mathbf{V}(x) \end{aligned}, \tag{7}$$

where $\mathbf{Z} = j\omega\mathbf{L}$, $\mathbf{Y} = j\omega\mathbf{C}$, $\mathbf{V}(x) = \left[V_G(x), V_R(x)\right]^T$ and $\mathbf{I}(x) = \left[I_G(x), I_R(x)\right]^T$. Solving (7) for terminal voltages we find

$$\frac{V_R(\mathsf{L})}{V_S/4} = \frac{\left[-\frac{j\omega l_m \mathsf{L}}{Z_0} + j\omega c_m \mathsf{L} Z_0\right] \cdot \frac{\sin(\beta\mathsf{L})}{\beta\mathsf{L}}}{\left(\cos(\beta\mathsf{L}) + j\frac{\sin(\beta\mathsf{L})}{\sqrt{1-k^2}}\right)^2} \tag{8}$$

and

$$\frac{V_R(0)}{V_S/4} = \frac{\left[\frac{j\omega l_m \mathsf{L}}{Z_0} + j\omega c_m \mathsf{L} Z_0\right] \cdot \frac{\sin(\beta\mathsf{L})}{\beta\mathsf{L}}}{\cos(\beta\mathsf{L}) + j\frac{\sin(\beta\mathsf{L})}{\sqrt{1-k^2}}} \tag{9}$$

where V_S is the open circuit voltage of the source. From (5) and (6) we obtain

$$\frac{l_m}{c_m} = Z_0^2 . \tag{10}$$

Substituting (10) into (8) and into (9) we have

$$V_R(0) = j\frac{V_S}{2}\sin(\beta\mathsf{L})\frac{k/\sqrt{1-k^2}}{\cos(\beta\mathsf{L}) + j\frac{\sin(\beta\mathsf{L})}{\sqrt{1-k^2}}} \tag{11}$$

and $V_R(\mathsf{L}) = 0$, respectively. The interpretation of (8) and (9) is immediate in the limit as $\beta\mathsf{L} \to 0$ (lumped model). In particular we see (note the different signs of the two terms within the square brackets in (8) and (9)), that $V_R(\mathsf{L}) = 0$ because the effects of magnetic (inductive) and electric (capacitive) coupling cancel out at $x = \mathsf{L}$ (while add in phase at $x = 0$). Due to imperfections in the practical realization of the directional coupler (due to the unavoidable asymmetries) this cancellation cannot be total. Note finally that $V_G(0) = V_S/2$ and

$$\frac{V_G(\mathsf{L})}{V_S/2} = \left[\cos(\beta\mathsf{L}) + j\frac{\sin(\beta\mathsf{L})}{\sqrt{1-k^2}}\right]^{-1} \tag{12}$$

The representation of the four-port network in terms of scattering parameters is now if interest, see Fig. 2.

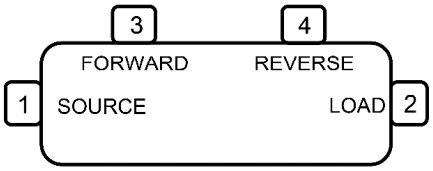

Figure 2. Schematic representation of a directional coupler

The port numbering is as follows: Port 1 – line G at $x = 0$, Port 2 – line G at $x = \mathsf{L}$, Port 3 – line R at $x = 0$, Port 4 – line R at $x = \mathsf{L}$. With this numbering the scattering matrix $\mathbf{S}$ is (consider that the network is reciprocal, then $\mathbf{S}$ is symmetric)

$$\mathbf{S} = \begin{pmatrix} 0 & S_{21} & S_{31} & 0 \\ S_{21} & 0 & 0 & S_{31} \\ S_{31} & 0 & 0 & S_{21} \\ 0 & S_{31} & S_{21} & 0 \end{pmatrix} \tag{13}$$

Coupled voltages are strongly frequency dependent hence practical use of directional couplers is narrowband about the frequency at which $\mathsf{L} = \lambda/4$. At such frequency we have, from (12), $S_{21} = -j\sqrt{1-k^2}$ and, from (11), $S_{31} = k$. It is evident from (13) that if a matched load is connected at port 2 then the power delivered to the load at port 3 is $|S_{21}|^2 P$, where P is the power delivered by the source to port 1, and the power delivered to port 4 is zero. If a load of complex reflection coefficient $\Gamma \neq 0$ is instead connected at port 2 then the power delivered to port 3 is again $|S_{21}|^2 P$ while the power delivered to port 4 is $|S_{21}|^2 |S_{31}|^2 P|\Gamma|^2$. It is therefore clear the operation of the coupler in splitting forward and reflected power toward port 3 and port 4, respectively. The parameters $|S_{21}|$ and $|S_{31}|$ are of great importance in the specification of directional couplers and take specific designations, when expressed in decibel, namely insertion loss (*IL*)

$$IL = -20\log|S_{21}| \tag{14}$$

and coupling (*C*)

$$C = -20\log|S_{31}| \tag{15}$$

The $\mathbf{S}$ matrix of a real (imperfect) directional coupler includes all the terms that in (13) are ideally zero, namely mismatch at the four ports (S_{11}, S_{22}, S_{33}, S_{44}), isolation between port 1 and port 4 (S_{41}) and between port 2 and port 3 (S_{32}). In addition to insertion loss and coupling other important parameters are introduced to specify the non-ideal behavior of the directional coupler, namely isolation (*I*)

$$I = -20\log|S_{41}| \tag{16}$$

and directivity (*D*)

$$D = -20\log\frac{|S_{41}|}{|S_{31}|} . \tag{17}$$

Note that

$$D = I - C . \tag{18}$$

The most critical mismatch is the return loss of port 2 (*RL*) given by

$$RL = -20\log|S_{22}|. \tag{19}$$

To evaluate complex reflection coefficient measurement accuracy a functional model is necessary linking the measurand with the parameters of the coupler that quantify non idealities. Such mathematical relationship can be derived from the scattering parameters as

$$\Gamma' = \frac{\Gamma + \frac{\Lambda}{\Delta}(1-\Gamma\Sigma)}{\frac{\Gamma}{\Delta} + \Lambda(1-\Gamma\Sigma)} \tag{20}$$

where Γ is the true (complex) reflection coefficient and Γ' is the measured (complex) reflection coefficient, obtained by ratioing the forward wave to the matched load at port 4 over the forward wave to the matched load at port 3. The other (complex) parameters appearing in (20) are $\Delta = S_{31}/S_{41}$, $\Sigma = S_{22}$ and $\Lambda = 1/S_{21}$, which are evidently related to directivity (17), return loss (19) and insertion loss (14), respectively. Inverting (20) we obtain

$$\Gamma = \Lambda \frac{\Gamma' - \frac{1}{\Delta}}{1 - \frac{\Lambda}{\Delta}\Sigma + \Gamma'\left(\Lambda\Sigma - \frac{1}{\Delta}\right)} \tag{21}$$

For a quasi-ideal directional coupler $|\Delta| \to \infty$ and $|\Sigma| \to 0$ then from (21)

$$\Gamma \to \Lambda\left[\Gamma' - \frac{1}{D} - (\Gamma')^2 \Lambda\Sigma\right]. \tag{22}$$

The correction for insertion loss and the errors due to directivity and mismatch can be immediately identified and in (22).

3 Directional Bridges

A directional bridge (or resistive coupler) is, similarly to a directional coupler, a reflectometer, i.e., a device that permits to discriminate the forward and the reflected waves. A wide-band reflectometer cannot be realized by use of a directional coupler whose bandwidth is of few octaves. A single directional bridge can instead cover several frequency decades, from few kilohertz up to several gigahertz. The use of directional bridges is then more convenient at low frequency, while directional couplers are more suitable at high frequency, starting from several hundreds of megahertz to microwaves.

Now, see Fig. 3. Let be $Z_0 = 50\,\Omega$, Z_X is the unknown test port impedance, The input impedance of the receiver (detector) is Z_0. The impedance of the source is Z_S and its open circuit voltage is V_S. The voltage across the detector (e.g., a spectrum analyzer) is

$$V_{BA} = V_D = \frac{Z_0(Z_X - Z_0)}{Z_X(3Z_S + 5Z_0) + Z_0(5Z_S + 3Z_0)} V_S. \tag{23}$$

If $Z_X = \infty$ then

$$V_D|_{Z_X=\infty} = \frac{Z_0}{3Z_S + 5Z_0} V_S. \tag{24}$$

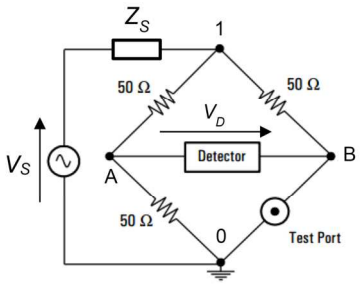

Figure 3. Electrical schematic showing the principle of operation of a directional bridge.

Normalizing V_D with respect to $V_D|_{Z_X=\infty}$ we obtain

$$\frac{V_D}{V_D|_{Z_X=\infty}} = \frac{(Z_X - Z_0)(3Z_S + 5Z_0)}{Z_X(3Z_S + 5Z_0) + Z_0(5Z_S + 3Z_0)}. \tag{25}$$

Finally, if $Z_S = Z_0$, we have

$$\frac{V_D}{V_D|_{Z_X=\infty}} = \frac{Z_X - Z_0}{Z_X + Z_0} = \Gamma. \tag{26}$$

The normalized voltage is the (complex) reflection coefficient Γ.

To prevent the test port arm of the directional bridge from being short-circuited by a single ended detector the voltage between node 1 and node 0 cab be provided by the secondary of a 1:1 radiofrequency transformer whose primary is fed by the source. This implies a low-frequency limit (corner frequency) $Z_0/4\pi L$, where L is the self-inductance of the primary and secondary coils. Another solution, different from a 1:1 transformer may be symmetrically tapping the voltage across the bridge diagonal with respect to ground through an identical couple of inductive chokes. In this case, a low corner frequency is introduced above which the magnitude of the choke impedance is high compared with Z_0. Asymmetries in the 1:1 transformer or in the chokes degrade the performance of the directional bridge in terms of directivity.

A directional bridge can be seen as a directional coupler in which port 3 is internally terminated, hence the remaining accessible ports are, see Fig. 2, port 1 (Source), port 2 (or Test Port, Load), port 4 (Detector, Reverse). The scattering matrix of the ideal directional bridge is (the detector port is numbered 3 from now on)

$$\mathbf{S} = \begin{pmatrix} 0 & 1/2 & 0 \\ 1/2 & 0 & 1/2 \\ 0 & 1/2 & 0 \end{pmatrix}. \tag{27}$$

It is immediate to verify that ratioing the forward wave to the detector when a load of reflection coefficient Γ is connected to port 2 over the forward wave to the detector when port 2 is left open we directly obtain Γ. In the case of a real bridge the isolation between the source and detector port and the return loss of the test port are not infinite (S_{13} and S_{22} are not zero). The ratio of the forward waves to the detector port in the load/no load (open) cases is the measured (complex) reflection coefficient Γ', given by

$$\Gamma' = \frac{\frac{1}{\Delta} + \frac{\Gamma}{1-\Gamma\Sigma}}{\frac{1}{\Delta} + \frac{1}{1-\Sigma}}, \tag{28}$$

where $\Delta = S_{21}S_{32}/S_{31}$ is the analogous of the directivity of the directional coupler ($1/S_{31}$ corresponds to the isolation, while $1/S_{21}S_{32}$ to the coupling) and $\Sigma = S_{22}$ is the mismatch of the test port. Inverting (28) we obtain

$$\Gamma = \frac{\Gamma'\left(\frac{1}{\Delta} + \frac{1}{1-\Sigma}\right) - \frac{1}{\Delta}}{1 + \Sigma\left[\Gamma'\left(\frac{1}{\Delta} + \frac{1}{1-\Sigma}\right) - \frac{1}{\Delta}\right]}. \tag{29}$$

For a quasi-ideal directional bridge $|\Delta| \to \infty$ and $|\Sigma| \to 0$ then from (29)

$$\Gamma \to \Gamma' - \frac{1}{D} - (\Gamma')^2 \Sigma. \tag{30}$$

Note that (22) and (30) are similar (identical if one takes $\Lambda = 1$).

4 References

1. C. F. M. Carobbi, M. Cati, C. Panconi, "Reproducibility of Radiated Emissions Measurements in Compact, Fully–Anechoic, Rooms — The Contribution of the Site-to-Site Variations," IEEE Trans. on EMC, vol. 51, no. 3, pp. 574-582, Aug. 2009.

2. C. F. M. Carobbi and L. M. Millanta, "Circuit Loading in Radio-Frequency Current Measurements: The Insertion Impedance of the Transformer Probes," IEEE Trans. on I&M, vol. 59, no. 1, pp. 200-204, Jan. 2010.

3. C. F. M. Carobbi, M. Cati, C. Panconi, "A Double Inequality for Equivalent Impulse Bandwidth," IEEE Trans. on EMC, vol. 52, no. 3, pp. 516-520, Aug. 2010.

4. C. F. M. Carobbi, M. Cati, C. Panconi, "Note on the Expected Value and Standard Deviation of the Mismatch Correction," IEEE Trans. on EMC, vol. 53, no. 4, pp. 1098-1099, Nov. 2011.

5. C. F. M. Carobbi and M. Stecher, "The Effect of the Imperfect Realization of the Artificial Mains Network Impedance on the Reproducibility of Conducted Emission Measurements," IEEE Trans. on EMC, vol. 54, no. 5, pp. 986-997, Oct. 2012.

6. C. F. M. Carobbi, A. Bonci, M. Stellini and M. Borsero, "Time-Domain Characterization of the Surge, EFT/Burst and ESD Measurement Systems," IEEE Trans. on Instrumentation and Measurement, vol. 62, no. 6, pp. 1840-1846, Jun. 2013.

7. C. F. M. Carobbi, "Measurement Error of the Standard Unidirectional Impulse Waveforms Due to the Limited Bandwidth of the Measuring System," IEEE Trans. on EMC, vol. 55, no. 4, pp. 692-698, Aug. 2013.

8. C. F. M. Carobbi and A. Bonci, "Elementary and Ideal Equivalent Circuit Model of the 1,2/50 – 8/20 μs Combination Wave Generator," IEEE-EMC Magazine, vol. 2, issue 4, pp. 51-57.

9. C. F. M. Carobbi, "Bayesian inference on a squared quantity," Measurement 48 (2014), pp. 13–20.

10. C. F. M. Carobbi, A. Bonci, M. Cati, C. Panconi, M. Borsero and G. Vizio, "Design, Preparation, Conduct and Result of a Proficiency Test of Radiated Emission Measurements", IEEE Trans. on EMC, vol. 56, no. 6, pp. 1251-1261, Dec. 2014.

11. C. Carobbi and F. Pennecchi, "Bayesian conformity assessment in presence of systematic measurement errors," Metrologia 53 (2016) S74–S80.

12. C. F. M. Carobbi, A. Bonci, M. Cati, C. Panconi, M. Borsero and G. Vizio, "Proficiency Testing by Using Traveling Samples with Preassigned Reference Values", IEEE Trans. on EMC, vol. 58, no. 4, pp. 1339 – 1348, Aug. 2016.

13. C. F. M. Carobbi, "Bayesian Inference in Action in EMC – Fundamentals and Applications", IEEE Trans. on EMC, vol. 59, no. 4, pp. 1114 – 1124, Aug. 2017.

14. Carlo Carobbi and Danilo Izzo, "Reproducibility of CISPR 25 ALSE Test Method", 2017 IEEE Int. Symp. on EMC, Washington (DC), Aug. 6-11, 2017.

15. C. F. M. Carobbi, "The Statistical Field Uniformity Criterion in Transverse Electromagnetic Waveguides," IEEE Trans. on EMC, vol. 59, no. 6, pp. 2052 – 2053, Dec. 2017.

16. C. F. M. Carobbi, and D. Izzo, "Evaluation and Improvement of the Reproducibility of CISPR 25 ALSE Test Method," IEEE Trans. on EMC, vol. 60, no. 4, pp. 1069 – 1077, Aug. 2018.

17. C. F. M. Carobbi, "A Lumped Model of the Rod Antenna Setup Adopted for Military and Automotive Testing," IEEE Trans. on EMC, vol. 61, no. 4, pp. 1289 – 1296, Aug. 2019.

18. C. F. M. Carobbi, S. Lalléchère, and L. R. Arnaut, "Review of Uncertainty Quantification of Measurement and Computational Modeling in EMC Part I: Measurement Uncertainty," IEEE Trans. on EMC, vol. 61, no. 6, pp. 1698 – 1705, Dec. 2019.

19. S. Lalléchère, C. F. M. Carobbi, and L. R. Arnaut, "Review of Uncertainty Quantification of Measurement and Computational Modeling in EMC Part II: Computational Uncertainty," IEEE Trans. on EMC, vol. 61, no. 6, pp. 1699 – 1706, Dec. 2019.

20. Ramiro Serra and Carlo Carobbi, "Bayesian inference on the parameters of the truncated normal distribution and application to reverberation chamber measurement data," Measurement Science and Technology, Volume 31, Number 7, 9 April 2020, https://doi.org/10.1088/1361-6501/ab7316.

21. Alessio Bonci, Enrico Boni, and Carlo F. M. Carobbi, "A Compact, Broadband, Calculable Electromagnetic Field Source for Quality Assurance in EMC Testing," IEEE Trans. on EMC, 2020, Early Access Article, https://doi.org/10.1109/TEMC.2020.3010578.

22. Clayton R. Paul, "Solution of the Transmission-Line Equations for Three-Conductor Lines in Homogeneous Media," IEEE Trans. on EMC, vol. EMC-20, no. 1, pp. 216-222, Feb. 1978.